Journal of Catalysis **181,** 223–232 (1999)
Article ID jcat.1998.2298, available online at http://www.idealibrary.com on IDEAL®

Preparation of Supported Gold Catalysts for Low-Temperature CO Oxidation via "Size-Controlled" Gold Colloids

Jan-Dierk Grunwaldt, Christoph Kiener, Clemens Wögerbauer, and Alfons Baiker[1]

Laboratory of Technical Chemistry, Swiss Federal Institute of Technology, ETH-Zentrum, CH-8092 Zürich, Switzerland

Received June 12, 1998; revised September 28, 1998; accepted September 29, 1998

Catalytically active gold model catalysts have been designed via "size-controlled" gold colloids of 2-nm mean particle size. They were prepared by reduction of chloroauric acid with tetrakis-(hydroxymethyl)phosphonium chloride in an alkaline solution, followed by adsorption of gold colloids on TiO_2 and ZrO_2 at a pH lower than the isoelectric point of the metal oxides. Investigation of the size of the gold particles in solution by UV-vis spectrophotometry in combination with HRTEM indicated that the gold colloids are rather stable in alkaline solution, during pH-change and purification with dialysis. Ageing of the solutions showed that the particle size slowly increased over a time scale of 4 months. Analysis of the dried catalysts by XRD and HRTEM corroborated that the particle size was nearly preserved during the immobilization process. Only in the case of high loadings (16.6 wt%, compared to the calculated nominal monolayer coverage of 45–55 wt%), incomplete adsorption occurred, affording more inhomogeneous dispersion and some aggregation. After calcination at 673 K, both zirconia- and titania-based catalysts containing 1.7 wt% Au exhibited high activity in low temperature CO oxidation. Although the particle size on both supports was comparable, the Au/TiO_2 catalyst showed significantly higher activity than the Au/ZrO_2 catalyst. The uncalcined Au/TiO_2 also exhibited high activity, whereas the uncalcined Au/ZrO_2 was inactive under the same conditions, corroborating that not only the gold particle size but also the support plays a key role in CO oxidation.

Key Words: **CO oxidation; gold catalysts; colloids; gold nanoparticles; immobilization; TiO_2; ZrO_2.**

1. INTRODUCTION

Gold nanoparticles deposited on metal oxides, such as TiO_2, ZrO_2, α-Fe_2O_3, Co_3O_4, and NiO, exhibit high activity in the low temperature oxidation of carbon monoxide (1–5), whereas the support alone, bulk gold and gold particles of about 20 nm in diameter are known to be rather inactive up to temperatures of about 573 K (6, 7). The catalytic performance of gold is supposed to depend markedly on particle size, the nature of the support, and the preparation methods. However, the interplay of the small gold particles with the support is not yet fully understood. One reason is that the final gold particle is formed on the support in most cases via a calcination step so that both the particle size and the support are interdependent, e.g. due to the different wetting ability of the metal oxide support during calcination. Hence, further insight into the role of the gold/metal oxide interface could be obtained by using "size-controlled" gold particles whose particle size is established before deposition on the metal oxide support.

One possible strategy to prepare size-controlled gold particles is the use of monodisperse gold sols. Frens *et al.* (8) reported the preparation of gold colloids in the range of 15–150 nm by reduction of chloroauric acid with sodium citrate. The tenfold difference in size could be produced by varying the amount of sodium citrate. For potential application in catalysis smaller gold particles need to be synthesized. The reduction of chloroauric acid with white phosphorus (procedure by Zigsmondy, quoted in (9)) or with tetrakis(hydroxymethyl)phosphonium chloride (10, 11) result in gold particles in the range of 2 nm.

Here we report the preparation of different supported gold catalysts via gold colloidal solutions using tetrakis(hydroxymethyl)phosphonium chloride as reducing agent. This preparation procedure is composed of the following steps: the preparation of the gold sol, its purification if necessary, immobilization on metal oxides in acidic medium analogous to metal complex anions, and finally, appropriate activation of the catalysts. To relate the final particle size on the support and the particle size in solution, emphasis was laid throughout all steps on the investigation of the structural properties, especially the stability of the gold particles.

2. EXPERIMENTAL

Preparation Procedures and Materials

A. Preparation of the gold sol. The gold sols were prepared similarly to the procedure reported by Duff *et al.* (10, 11) using $HAuCl_4 \cdot xH_2O$ from Fluka assayed at >49% gold by weight and tetrakis(hydroxmethyl)phosphonium chloride ($P(CH_2OH)_4Cl$, referred to hereafter as THPC)

[1] Corresponding author. E-mail: baiker@tech.chem.ethz.ch.

0021-9517/99 $30.00

from Fluka as 80% aqueous solution. NaOH and H_2SO_4 were diluted to specific concentrations from Titrisol standard solution ampoules (Merck). All solutions were made up with doubly distilled water.

In order to prepare 10 mg Au stabilized as colloid, the following sol preparation was performed: In a carefully cleaned round-bottomed flask containing 46.3 ml continuously stirred water, 1.5 ml 0.2 *M* NaOH, 1.0 ml THPC (1.2 ml of 80 wt% THPC in water diluted to 100 ml) and after 2 min 1.2 ml 43 m*M* $HAuCl_4$ solution were added. While pouring the gold(III) solution into the alkaline THPC-mixture, the solution changed in colour from light yellow to dark orange brown, indicating the formation of the gold sol.

B. Purification by dialysis and stability with mineral acids. To remove dissolved species, e.g. Na^+, OH^-, Cl^-, THPC, and reaction products, extensive dialysis was performed. For this purpose, a dialysis tubing (Sigma Aldrich, benzylated cellulose, 20 mm diameter, <12000 u) was used, cleaned by boiling and subsequent rinsing with water for 3 days before use. 50-ml gold sol was purified for 2 days in 2 liters water with threefold change of water. To investigate the stability during pH-change and the possible aggregation of the fresh colloid and of the corresponding dialyzed solution, they were acidified with 2 *M* H_2SO_4. Stability of the gold colloids over a longer time period was investigated by keeping it for a definite time (1 day, 1 week, 2 months, 4 months) in a closed vessel prior to analysis.

C. Immobilization on metal oxide supports. The commercially available oxides TiO_2 (Degussa P25), Al_2O_3 (Alumina C, Degussa), and ZrO_2 (Degussa) were suspended in water (0.2–1.0 wt%, pH = 2) by ultrasonic treatment (15 min). While stirring, ca 50 ml of an H_2SO_4-treated solution (pH = 2) with gold nanoparticles (10-mg Au, as described above) was added. Dialyzed and nondialyzed gold sols were used. After 10 min the suspension was filtered by vacuum filtration through a cellulose filter membrane of 0.45-mm pore size and washed three times with water. Finally, the remaining solid was dried at 323 K *in vacuo* for 15 h. The filtrate was investigated by UV-vis spectrophotometry to check if adsorption was complete. An overview of the prepared samples and their different characteristics is given in Table 1. The following abbreviations are used. "P" stands for the powder sample, "Au" stands for loading with gold, "Ti" or "Zr" denotes the support which was used, "D" means that the sol was dialyzed before adsorption and the numbers 1.7 and 17 are used to indicate the loading (rounded values). All samples were stored under air for a longer period (>7 days) before further characterization and catalytic testing.

TABLE 1

Overview on the Samples Prepared by Adsorption of Gold Colloids on Different Oxide Powders

Sample	Support	Nominal loading of Au in wt%	BET m^2/g	IEP	pH	Dialysed	BET after reaction m^2/g
PAuTi1.7	TiO_2	1.7	60	6	2	N	42
PAuTiD1.7	TiO_2	1.7	60	6	2	Y	—
PAuTi17	TiO_2	16.6	60	6	2	N	—
PAuTiD17	TiO_2	16.6	60	6	2	Y	—
PAuZr1.7	ZrO_2	1.7	40	6.7	2	N	32
PAuZrD1.7	ZrO_2	1.7	40	6.7	2	Y	—
PAuZr17	ZrO_2	16.6	40	6.7	2	N	—
PAuZrD17	ZrO_2	16.6	40	6.7	2	Y	—

Catalyst Characterization

UV-vis spectrophotometry. UV-vis spectra of the samples were recorded with a Perkin Elmer Lambda 16 ultraviolet-visible spectrometer at wavelengths between 900 and 200 nm in quartz cells (0.5-cm path length) after 1 : 16 dilution of the sols. Water was used as a reference.

HRTEM. High resolution transmission electron microscopic investigations (HRTEM) were carried out using a Phillips CM30ST electron microscope with CeB6-cathode and a Jeol 2010 electron microscope with LaB6-cathode at an accelerating voltage of 300 kV and 200 kV, respectively. In the case of colloidal solutions, the gold sol was directly dropped onto the carbon-coated grid and used for investigations. The powder catalysts were suspended in ethanol for about 1 min under ultrasonic treatment before depositing them on the carbon support. The mean particle diameter $\langle dp \rangle$ was calculated from the mean diameter frequency distribution with the formula

$$\langle dp \rangle = \frac{\sum n_i \cdot dp_i}{\sum n_i},$$

where $\sum$ is the sum of i over the whole sample, n_i the number of particles with particle diameter dp_i in a certain range. The corresponding root mean square error σ was calculated using the following statistical expression:

$$\sigma(dp) = \sqrt{\frac{\sum n_i \cdot (\langle dp \rangle - dp_i)^2}{\sum n_i - 1}}.$$

XRD. X-ray diffraction of the supported gold particles was performed on a Siemens D 5000 powder X-ray diffractometer. Diffraction patterns were recorded with detector-sided Ni-filtered Cu Kα radiation (40 mA, 40 kV) over a 2θ-range of 2° to 70° and a position-sensitive detector using a step size of 0.010° and a step time of 2.5 s. Measured patterns were compared with JCPDS data files (12). The mean crystallite sizes were estimated using the Scherrer equation (13, 14) and the peaks of selected reflections in the diffraction pattern, which were fitted by a Gaussian function.

Peak broadening due to the instrumental broadening of $2\theta = 0.08^\circ$ was taken into account.

XPS. The surface composition was examined by XPS performed in a Leybold Heraeus LHS 11 MCD instrument. Mg Kα radiation was used to excite photoelectrons which were analyzed with the analyzer operated at 150 eV pass energy at an energy scale calibrated versus Au $4f_{7/2}$ at 84.0 eV. The surface composition of the samples was determined from the peak areas of the corresponding lines using a Shirley-type background and empirical cross section factors for XPS (15, 16).

Surface areas. BET surface areas (S_{BET}) were obtained by physisorption of N_2 at 77 K using a Micromeritics ASAP 2000 instrument. Prior to measurement, the samples were outgassed to 0.1 Pa at 363 K. S_{BET} were calculated in a relative pressure range between $0.05 < p/p_0 < 0.2$, assuming a cross-sectional area of 0.162 nm^2 for the N_2 molecule (17).

Catalytic tests. Steady-state catalytic tests were carried out in a continuous flow fixed-bed microreactor. The powder was embedded between glass wool plugs in an 8 mm ID glass reactor tube. Experiments in the temperature range 250 K–450 K and at atmospheric pressure were performed using 200-mg catalyst. Prior to activity tests the catalyst was dried in a constant Argon stream at room temperature until no more water was released (>2 h). The reaction mixture, containing 2500 ppm CO (99.997%, Pangas) and 2500 ppm O_2 (99.999%, Pangas) in a nitrogen balance was dried by a cooling trap. Standard experiments were performed using a CO feed rate of 2.5×10^{-7} mol $\cdot s^{-1} \cdot g_{cat}^{-1}$. The gas hourly space velocity amounted to ca 12000 h^{-1}. Kinetic data were taken after 20 min on stream at specified conditions.

Products were analyzed either by a gas chromatograph (HP, model 5890A) equipped with a Poropak QS column (5 m in length, 1/8-in. diameter) and a TCD or with an FTIR spectrometer Bruker IFS 66 with heatable gas cell (3.2 m optical path length, gold coated mirrors, ZnSe windows, and 100 ml volume). For further details see Refs. (18, 19).

3. RESULTS

Characterization and Stability of Gold Colloids in Solution

The reduction of chloroauric acid with THPC resulted in a dark orange-brown sol within a few seconds after mixing. The sol did not change its consistency and colour after ageing for a few days or dialysis and increasing acidity to pH = 2. Only after 2–3 months did the the colour of the solution change to a slightly reddish colour.

For more detailed analysis of the particle size and the stability of the gold colloids, optical spectrophotometry in combination with HRTEM was used. From earlier studies it is known that the maximum of the extinction band in UV-vis spectrophotometry is a function of particle size of the small metal particles (20–22), which can be described by the scattering theory for spheres (23, 24). Typical UV-vis spectra of gold colloids with different particle sizes after different ageing times are shown in Fig. 1.1. Some of the corresponding HRTEM-images are depicted in Figs. 1.2 to 1.4. The freshly prepared solution exhibits due to finite size effects (21, 22) only a broad extinction band around 500 nm (Fig. 1.1a) in the UV-vis spectrum and a gold particle size around 2 nm (Figs. 1–2) in HRTEM. The intensities of the extinction band of the other solutions increase and the maximum is shifted to higher wavelengths (Figs. 1.1b to 1.1d). This is accompanied by an increase of the particle size (3–4 nm in Figs. 1.3 and 5–6 nm in Fig. 1.4). HRTEM also uncovers that such small particles are ordered showing typical Au(111) fringes of 0.236 nm apart from each other. The HRTEM results were recently corroborated by small angle X-ray scattering measurements.

This shows that UV-vis spectrophotometry can be used *in situ* to monitor changes in the gold particle size. Therefore it has been applied for studies of the stability of the gold colloids during purification steps and pH change in this paper. Figure 1 additionally gives a detailed picture on the stability of the gold colloids. After one week the optical extinction band increased only partly, after two months the as-prepared gold colloids increased in size by a factor of 2 and were still stable in solution.

Typical UV-vis spectra at different stages of the hydrosol preparation are depicted in Fig. 2 showing that purification of the hydrosol by dialysis only slightly affects the extinction band around 200 nm but not significantly the plasmon excitation band around 500 nm (Fig. 2c). Hence, the gold colloids do not aggregate significantly and the particle size is predominantly in the range of 2 nm. Figure 2 also shows the behaviour of the gold sols during pH-change. Acidifying with H_2SO_4 did not effect change in colour, the optical extinction spectrum remained the same (Figs. 2b and 2d) and also the particle size in HRTEM remained in the same range. Small variations of the extinction at low wavelengths could be due to pH-dependent absorbance of the organic residue. Acidified solutions were only stable for limited periods, and a brown precipitate formed after a few days.

Hence, the small and rather stable gold colloids of the freshly prepared gold sol with a mean particle diameter of about 2 nm are useful precursors for gold catalysts. The colloidal particles can be immobilized on different supports, similar to complex anions in acidic solution.

Adsorption of Gold Colloids on Metal Oxide Supports

The next step consisted in preserving the particle size during immobilization on the metal oxide support. Addition of the acidified (pH = 2) dark orange-brown gold sol to a suspension of TiO_2 or ZrO_2 (pH = 2) produced a grey-brown suspension within a few seconds. Starting from 10 mg gold and 600 mg of the considered oxide (PAuTi1.7,

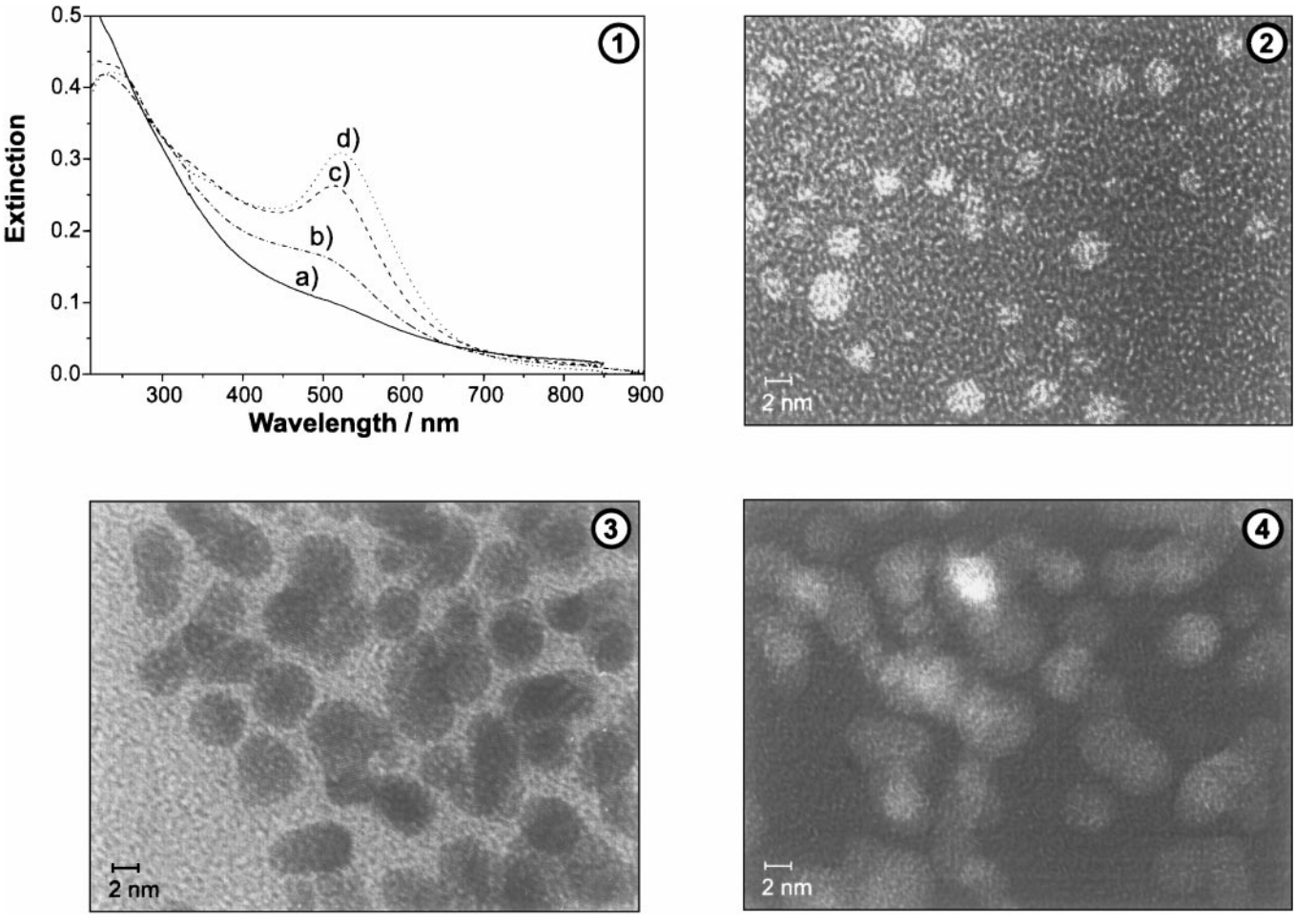

FIG. 1. (1) Optical extinction spectrum of a colloidal gold solution: (a) immediately after preparation; (b) after 1 week; (c) after 2 months; (d) after 4 months. (2) HRTEM image of the gold particles corresponding to spectrum 1a (ca 12 h after preparation). (3) HRTEM image of the gold particles corresponding to spectrum 1c (2 months after preparation). (4) HRTEM image of the gold particles corresponding to spectrum 1d (4 months after preparation).

PAuTiD1.7, PAuZr1.7, and PAuZrD1.7), the gold colloids were fully adsorbed on the support. The colourless filtrate did not show any band in the UV-vis extinction spectrum in the range of 300–800 nm any more. However, in the case of higher nominal loadings of gold (17 wt%), some differences between the oxide support, the crude and the purified gold sol were noted. Taking 10-mg gold and 60-mg TiO_2 (PAuTi17), the filtrate was also colourless and the UV-vis extinction spectrum indicated that almost no gold remained in solution. In the case of 10-mg gold on 60-mg ZrO_2 (PAuZr17), the UV-vis extinction spectrum of the filtrate still showed a band around 500 nm, as shown in Fig. 3b, and the filtrate remained brownish. The remaining gold particles could be fully adsorbed on an additional quantity of 60-mg ZrO_2 (Fig. 3c). Compared to the undialyzed gold sol, the adsorption of dialyzed colloidal gold solutions were incomplete on ZrO_2 and TiO_2, the adsorption capacity again being higher on TiO_2.

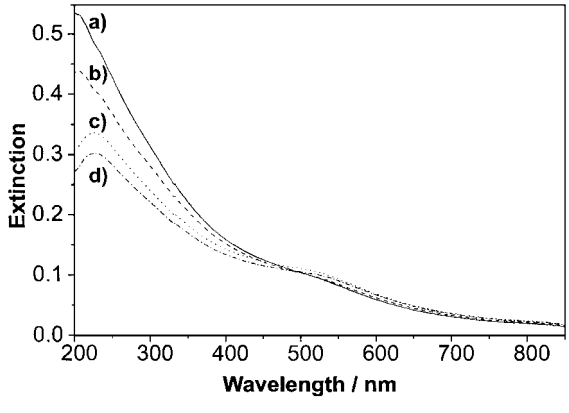

FIG. 2. UV-vis spectra of: (a) fresh colloidal solution; (b) fresh colloid, acidified to pH = 2; (c) colloidal solution after dialysis; (d) after dialysis, acidified to pH = 2.

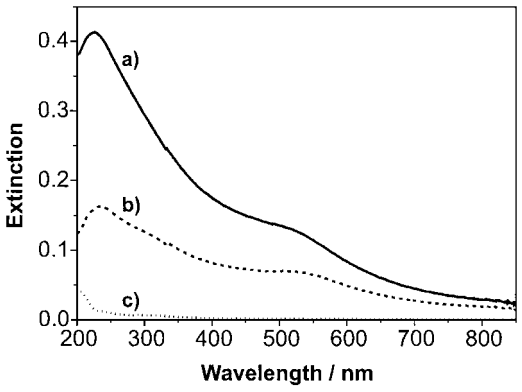

FIG. 3. UV-vis extinction spectrum of: (a) fresh dialyzed gold sol; (b) filtrate after incomplete adsorption on 60 mg ZrO_2; (c) filtrate after complete adsorption in a second step.

These results, obtained from UV-vis spectrophotometry, are also reflected by the surface composition of the gold supported oxide materials in XPS-studies, summarized in Table 2. For better comparison of the samples, the theoretical ratio of the gold surface Au_{surf} to the BET surface area of the support (see Table 2), denoted here with A_0, was calculated, assuming that the surface is covered by spherical gold particles of 2.0-nm diameter as determined by HRTEM before (Fig. 1). The data of two types of catalysts—one with higher nominal loading (17 wt%) and one with lower nominal loading (1.7 wt%)—are listed. Comparing the 1.7 wt% loaded catalysts PAuTi1.7, PAuTiD1.7, PAuZr1.7, and PAuZrD1.7, the samples exhibit only small differences between the n(Au)/n(Au + Ti) and n(Au)/n(Au + Zr) surface ratios. The value of zirconia containing samples is slightly higher because the ZrO_2 surface area is lower, which is reflected by data in the last column.

More differences are found for the higher loaded samples. Comparison of samples PAuTi17 and PAuZr17 indicates that the gold coverage is lower on zirconia. These findings corroborate the results from UV-vis spectrophotometry, where some gold colloids were found to remain in the filtrate. Some more insight is provided by columns 6 and 7 in Table 2. Both the calculated value and the ratio determined by XPS increase by a factor of 10 in the case of titania, showing that almost all gold colloids were adsorbed. However, in the case of zirconia this ratio increases only by about 8 times, indicating incomplete adsorption of gold. In the case of the dialyzed samples (PAuTiD17 and PAuZrD17), the increase, compared to lower loaded samples is even less: a factor of 6 in the case of the titania support and a factor of 2.5 in the case of zirconia. These results again corroborate the observations from UV-vis spectrophotometry, underlining that the loading on titania is higher.

Concerning impurities, which can also be uncovered by XPS, a significant amount of carbon impurity was found, as illustrated in column 2 of Table 2. It has to be noted that some of the carbon impurities originated from the sample holder. The carbon impurities varied to a large extent and seemed to be dependent on factors other than only dialysis. Sodium and phosphorous impurities were small, and due to the small sensitivity factors of both elements (15), no uniform tendency was found.

Structure of Gold Particles Deposited on Oxide Powders

To determine the structure and morphology of the gold particles in further detail, the samples were investigated with XRD and HRTEM, giving global and local information. A typical series of XRD patterns for the Au/TiO_2 system is shown in Fig. 4. Figures 4a and 4b represent the XRD-pattern for PAuTi17 and PAuTi1.7. Comparison with the pattern of pure titania (Fig. 4c) reveals that most of the reflections stem from the support TiO_2 P25 (anatase and rutile). The reflections for polycrystalline gold are expected at $2\theta = 38.2^\circ$ (100%), 44.4° (52%), 64.6 (32%), 77.4° (36%), etc., but they are not discernible in the

TABLE 2

Surface Composition of the Samples after Adsorption of Gold Colloids on Different Metal Oxides

Sample	C 1s in at%	O 1s in at%	Zr 3d or Ti 2p in at%	Au 4f in at%	n(Au)/n(Au + Ti); n(Au)/n(Au + Zr)[a]	Calculated value Au_{surf}/A_0[b]
PAuTi1.7	12.0	66.9	20.5	0.6	0.028	0.011
PAuTi1.7D	14.6	66.2	18.6	0.6	0.031	0.011
PAuTi17	18.8	61.1	14.6	5.5	0.27	0.11
PAuTiD17	15.7	61.7	18.7	4.0	0.18	0.11
PAuZr1.7	11.2	66.5	21.6	0.7	0.031	0.016
PAuZrD1.7	9.2	66.7	23.3	0.8	0.033	0.016
PAuZr17	21.4	57.2	16.3	5.1	0.24	0.16
PAuZrD17	13.2	65.9	19.3	1.6	0.077	0.16

[a] Derived from XPS-results by calculating the amount of gold referring to gold and titanium together on the surface.

[b] Coverage of the surface calculated from the gold loading (2.0-nm spherical particles) and the surface area of the support A_0 from BET measurements.

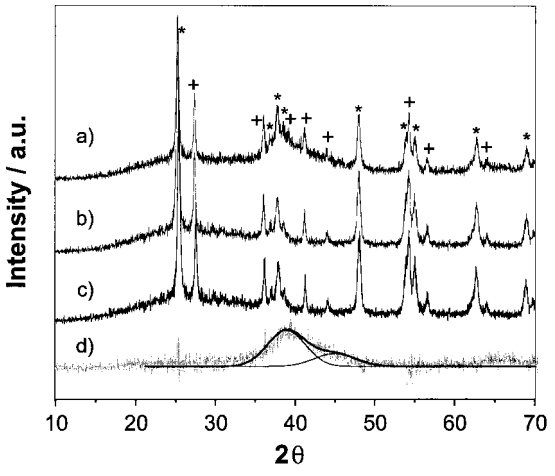

FIG. 4. XRD-pattern of Au colloids deposited on TiO_2 with + rutile, ∗ anatase: (a) Au on TiO_2 P25 (PAuTi17); (b) Au on TiO_2 P25 (PAuTi1.7); (c) TiO_2 P25; (d) difference spectrum (a)–(c). Some broad features remain around $2\Theta = 40^\circ$ and 65°, the fit of two Gaussian curves for the {111} and {200} reflections of gold.

XRD-patterns of Au/TiO_2. The parallel investigation of Au/ZrO_2 samples uncovered that also in this case the gold crystallites are very small, and strong line broadening occurs so that no distinct gold reflections are visible in the patterns. After subtraction of the pure TiO_2 XRD pattern from that of the higher Au loaded sample PAuTi17, some broad reflections remain around $2\theta = 40^\circ$ and $2\theta = 65^\circ$, as illustrated in Fig. 4d. Taking the 2θ values of the gold reflections at 38.2° and 44.4° into account, two Gaussian curves could be fitted as also depicted in Fig. 4d with a linewidth of 4.8° and 5.3° (in the 2θ scale), respectively. Assuming that the gold particles are spherical, one obtains according to Scherrer's equation a crystallite size of about 2.0 and 1.8 nm, respectively.

It appears that following deposition the gold particles nearly retain their initial particle size width of $\langle d \rangle = 2.0$ nm. The standard deviation is rather large because of the small particle size. A similar result is obtained for the zirconia-supported gold sample PAuZr17 by subtraction of the zirconia spectrum and the described fitting procedure. In the case of lower gold loadings (PAuTi1.7 and PAuZr1.7), the signal to noise ratio is too low, due to strong line broadening and their smaller concentration, so that the gold reflection is not strong enough in intensity.

Complementary information was obtained from HRTEM images. Typical HRTEM micrographs of low and high loaded TiO_2 and ZrO_2 are shown in Figs. 5.1 to 5.4. The gold particles are regularly distributed on the whole support. The particle size and morphology on PAuZr1.7 and PAuTi1.7 are very similar. The mean particle size was calculated from the particle size distribution in the TEM micrographs, which is illustrated in Fig. 5; the resulting mean particle sizes is summarized in Table 3. From the particle size distributions it is obvious that most particles are in the range of 1–2 nm, if the loadings are around 1.7 wt%. Since particles below 1 nm are difficult to monitor due to the low mass and diffraction contrast with respect to the support, the mean diameter which is given in Table 3 is probably too much influenced by larger particles. From the electron micrographs of higher loaded ZrO_2 and TiO_2 samples it follows that the distribution is not as homogeneous as in PAuZr1.7 and PAuTi1.7. Moreover, partial aggregation, which cannot be avoided during deposition, results in a slightly higher mean particle size (around 2.5 nm for PAuTi17). In most cases, separation between the gold clusters is maintained, but comparing several micrographs revealed that the particle size in the higher loaded samples PAuTi17 and PAuZr17 is locally different. In Fig. 5.4, a section with larger gold particles is depicted. They are significantly larger than the mean particle diameter from HRTEM and that which was calculated from XRD. Hence, the catalysts with lower loadings were used for further investigations. During the following steps (calcination in air to 673 K, or catalytic testing) only a small increase of the particle size was found with HRTEM; however, if they were heated to more than 673 K, particles >5 nm formed.

Catalytic Activity of Gold Particles Deposited on TiO_2 and ZrO_2

A. Dried (uncalcined) catalysts. For the investigation of the catalytic activity and the comparison of zirconia- and titania-supported catalysts, the 1.7 wt% loaded samples were used after drying at 323 K *in vacuo* and subsequent storage in air. Heating of the catalysts in the diluted reaction gas mixture containing a 1 : 1 mixture of carbon monoxide and oxygen interestingly revealed for the Au/TiO_2 catalyst 21% CO conversion at 305 K and full conversion at 353 K. In contrast, the uncalcined Au/ZrO_2 sample did not show any activity in CO conversion up to 353 K. Treating the Au/TiO_2 sample for 40 min at 423 K (100% conversion) resulted in a markedly more active catalyst at room temperature. Full conversion was measured down to 322 K and 90% conversion at 308 K. After 24 h, the conversion at 304 K was still 68% compared to only 21% at 305 K before heating. Using higher oxygen concentrations in the feed gas

TABLE 3

Mean Particle Size $\langle dp \rangle$ of Gold from HRTEM Micrographs at Different Au Loadings

Sample	Nominal Au loading in wt%	Support	$\langle dp \rangle$ in nm	$\sigma(\langle dp \rangle)$ in nm
PAuTi1.7	1.7	TiO_2	2.0	0.83
PAuTi17	16.6	TiO_2	2.5	0.94
PAuZr1.7	1.7	ZrO_2	1.9	1.0
PAuZr17	16.6	ZrO_2	2.6	0.84

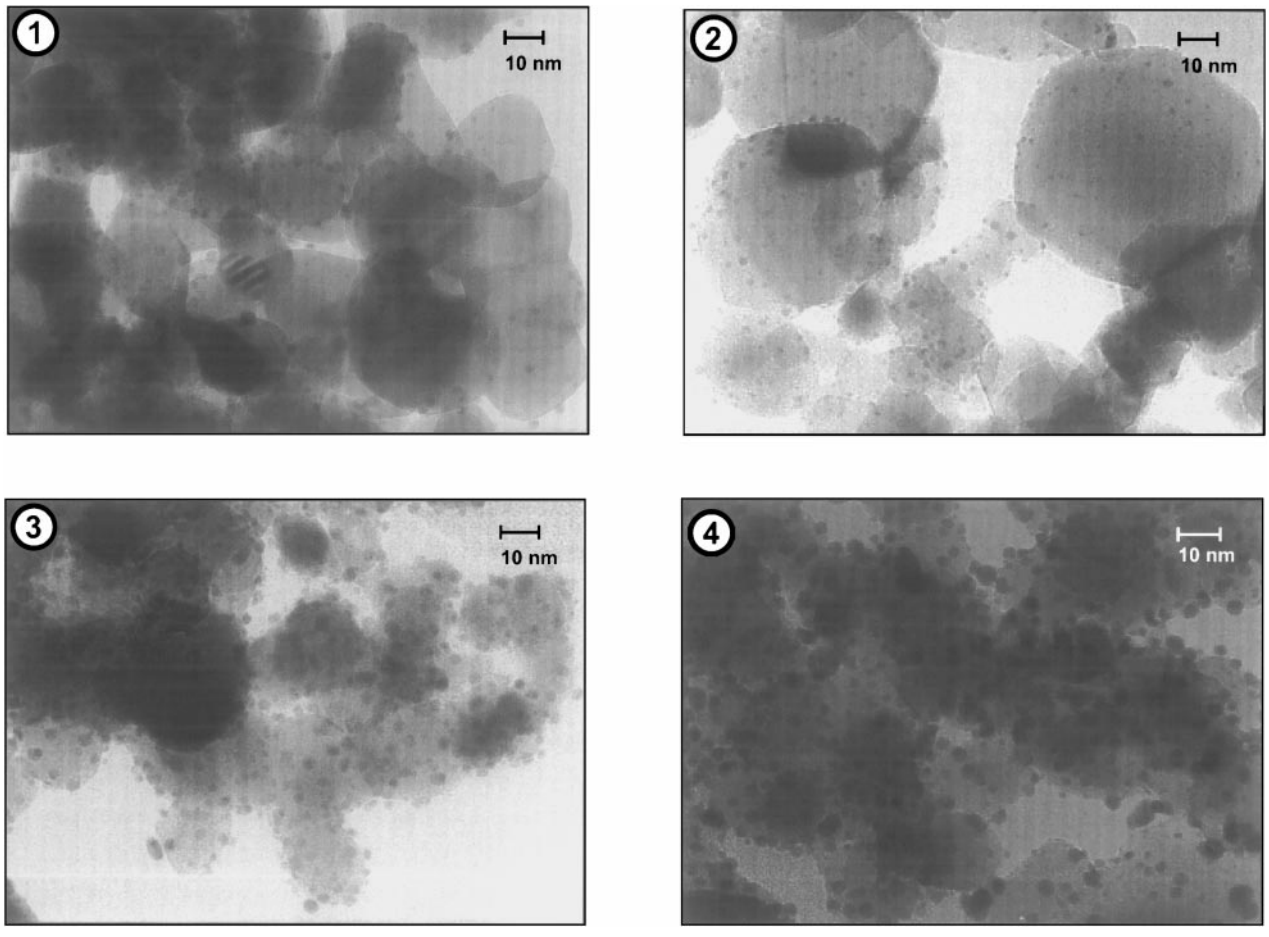

FIG. 5. High-resolution TEM micrographs of: (1) gold on zirconia (1.7 wt%, PAuZr1.7); (2) gold on titania (1.7 wt%, PAuTi1.7); (3) gold on zirconia (17 wt%, PAuZr17); (4) gold on titania (17 wt%, PAuTi17).

(20 vol%) the catalyst showed 100% conversion at room temperature.

B. Calcined catalysts. Since most gold catalysts, prepared up to now, were mostly activated in oxygen at 573–673 K before use, we applied a similar calcination procedure, also, to compare the activity of our catalysts to those prepared before. The catalytic activity of Au/ZrO_2 (1.7 wt% Au) and Au/TiO_2 (1.7 wt% Au), calcined at 673 K and cooled to room temperature in argon, was investigated between 250 K and 450 K. After an initial period to reach steady state, the catalytic activity was stable for several hours. The behaviour of both catalysts in CO oxidation in a 1 : 1 O_2/CO gas mixture and a CO feed of 2.5×10^{-7} $mol \cdot s^{-1}$ g_{cat}^{-1} is depicted in Fig. 6 as a function of temperature for different measurement conditions. Compared to the dried sample, calcined Au/ZrO_2 was significantly more active, showing 15% conversion at room temperature, attaining 50% conversion at ca 350 K, and full conversion at ca 400 K (Fig. 6a). Cooling the catalyst in the reaction mixture in the reversed cycle, starting at 473 K, resulted in lower overall activity (Fig. 6a). Further treatment of the catalyst for one day at 298 K under reaction conditions (10% CO conversion) and subsequent heating to 473 K afforded a similar activity behaviour in the cooling cycle as evidenced by the data in Fig. 6a, indicating that no further deactivation occurred. Note that the observed differences in activity are not only effects of activation/deactivation phenomena, because small differences in temperature around 298 K resulted in notable differences in activity.

For calcined gold/titania samples the temperature for 50% CO conversion was reduced slightly, compared to the dried sample, whereas full conversion was achieved at similar temperatures. The activity data shown in Fig. 7b reflect the steady state behaviour of Au/TiO_2 upon increasing the temperature after a preceding heating/cooling cycle. Note that full CO conversion was initially obtained by exposing the freshly calcined catalyst to reaction conditions at 298 K (not shown). If the catalyst was treated at higher temperatures and afterwards at lower temperatures (∼260 K), this resulted in the stable activity behaviour depicted in Fig. 7b with about 70% CO conversion at 298 K. Nearly the same conversion was obtained if the gas mixture was cooled back from 373 K (cooling 1); however, a higher activity was

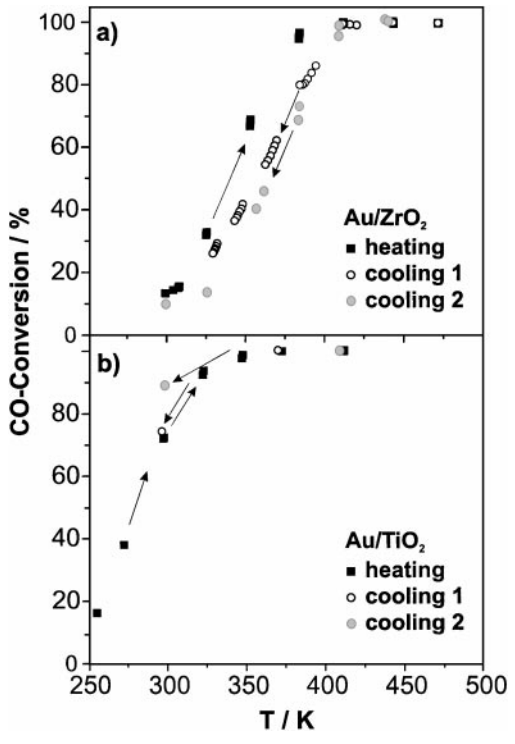

FIG. 6. CO oxidation of Au/MeO_2 catalysts containing 1.7 wt% of gold; dark squares represent CO conversion measured at increasing temperature and open circles at decreasing temperatures. Note that the hystereses were measured after different states (history) of the catalyst. With Au/ZrO_2 (a) the hysteresis shown represents an initial heating cycle and the first and second (after 1 day at 300 K in the reaction mixture) cooling cycle, whereas with Au/TiO_2 (b) a heating cycle after reaching equilibrium and a cooling cycle after heating to 373 K and 423 K are shown; conditions: 200 mg catalyst, total flow rate 30 $cm^3 \cdot min^{-1}$, 2500 ppm O_2, 2500 ppm CO, balance nitrogen.

obtained if the catalyst was heated to 423 K under reaction condition (cooling 2).

The influence of water on the catalytic activity was very pronounced at room temperature in the case of Au/TiO_2.

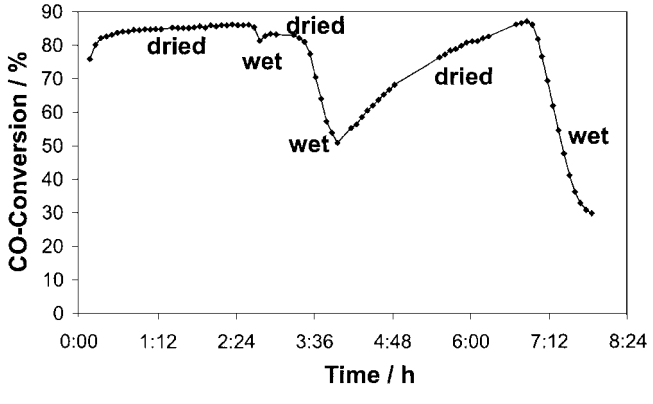

FIG. 7. Influence of water on the activity of Au/TiO_2 in CO oxidation at 298 K with dried and wet gas mixtures of CO and O_2; the conditions were 200 mg catalyst, total flow rate 30 $cm^3 \cdot min^{-1}$, 2500 ppm O_2, 2500 ppm CO, balance nitrogen.

The behaviour is shown for gold on titania at 298 K in Fig. 7. If the dried feed gas was changed to a slightly wet O_2/CO gas mixture (same gas mixture without a cooling trap, ca 0.1% H_2O, as estimated from the FTIR signal) the extent of CO-oxidation decreased significantly. This process was shown to be reversible. After switching the feed back to the dry gas mixture the activity increased notably and CO conversion gradually reached its initial value (Fig. 7).

4. DISCUSSION

The preparation of size-controlled gold particles and their deposition on metal oxide supports afforded a new type of active catalysts for the low temperature CO-oxidation. The initial size of the gold colloids was shown to be nearly preserved through all steps of the preparation. Before discussing the catalytic properties some important features of the preparation of the catalysts will be addressed.

Behaviour of Gold Sols after Reduction of $HAuCl_4$ with THPC

A crucial requirement for the activity of gold catalysts is the small gold particle size and its stability during purification and pH-change. These features were investigated in detail with UV-vis spectroscopy, which is very sensitive to changes in particle size, by comparison with HRTEM. Reduction of $HAuCl_4$ with THPC afforded gold particles of about 2 nm in size, similar to results of Duff *et al.* (11). This gold particle size is much smaller than that generally obtained with the conventional preparation procedure involving reduction with sodium citrate (8). The detailed analysis of the stability showed that neither dialysis nor pH change affected significantly the particle size. The particles are probably stabilized by a layer of adsorbed ligands, as emerged from XPS measurements which showed higher carbon and phosphorous contents than the pure support, even after dialysis. The adsorbed layer is probably destroyed during deposition or exposure to air. This explains that the gold particle size could be nearly preserved throughout these preparation steps. Ageing of the solutions was shown to be one possibility to prepare gold sols of different gold particle size. Another method, which is less time consuming, is boiling of the solutions as described by Duff *et al.* (11) or the admixture of other reducing agents. Note that HRTEM images clearly indicate that the gold colloids start to be crystalline in colloidal solution, as indicated by the resolved Au(111) fringes.

Adsorption of Gold Colloids on Metal Oxide Supports

Investigation of the adsorption of gold colloids showed that at pH = 2 gold colloids could be immobilized on the metal oxide surface as is known for metal complex anions (25, 26). The pH value is significantly lower than the isoelectric point of TiO_2 (IEP $\sim$ 6) and ZrO_2 (IEP $\sim$ 6.7) (25, 27).

The gold colloids can be assumed to be negatively polarized due to remaining chloro-ligands (28). Hence, the adsorption can be described by the electrostatic interaction with the positively charged surfaces. Adsorption on TiO_2/Au(111) and ZrO_2/Au(111) plates and their investigation with XPS has shown that Au colloids are preferentially adsorbed at pH < IEP and that at pH > IEP, additionally, Na^+ is adsorbed in significant quantities.

The adsorption of the gold colloids has been found to be complete in the case of low loading (1.7 wt%); however, in the case of higher loadings incomplete adsorption, especially in the case of zirconia occurred, as revealed by UV-vis spectrophotometry and XPS. Assuming that gold particles are spherical and 2 nm in diameter (as indicated by HRTEM), the calculated maximal gold loadings for titania and zirconia amount to 55 wt% and 45 wt%, respectively. These values are much higher than the nominal value of 17 wt% of the higher loaded samples. However, two additional factors have to be considered as well: (i) the gold particles are negatively polarized and are supposed to repel each other; (ii) the number of surface hydroxyl groups plays an important role which is known to depend on the kind of support and the pretreatment (29). This could be the reason that the gold adsorption capacity of zirconia is limited to ca 15 wt%. Interestingly, it was found that dialyzed gold particles adsorbed to a lower extent on both oxide surfaces. This shows that besides the electrostatic interactions additional factors (e.g., van der Waals interactions) due to the larger particle size could also play a role during the adsorption process.

Finally, it is worth mentioning that using the same procedure, alumina-supported gold catalysts could be prepared, corroborating that the range of suitable support materials can be easily extended. The immobilization of small gold particles on alumina is difficult to achieve by conventional impregnation and ion exchange techniques.

Structure of the Immobilized Gold Particles

The identification of the structure of the gold particles on titania and zirconia revealed that the gold particle size can be nearly preserved if the nominal loading amounts to 1.7 wt%. Also in the case of 16.6 wt% nominal loading, the particle size did not increase significantly. Hence, the reflections of the gold crystallites in XRD are very broad. HRTEM shows that to some extent agglomeration of the gold particles occurs. Also some inhomogeneities were observed. However, the particle size is still around 2.5 nm.

Similarity of the gold particle size on zirconia and titania provides the opportunity to compare directly the effect of different supports. Up to now, in most cases the final gold particle size was formed after immobilization on the support during calcination in air at 573 K and 673 K. The gold colloid route provides the opportunity to tune the final gold particle size before the support is involved by using "size-controlled" gold particles in solution. Ageing of the gold colloids, boiling of the sols, and different reducing agents can afford gold sols with different particle sizes.

Activity in Low Temperature CO Oxidation

An intriguing result of the present work is that gold deposited as a colloid on metal oxide supports is active for low temperature CO oxidation. Even the dried Au/TiO_2 catalysts are active without further calcination. It cannot be completely excluded that during the drying process some structural changes occur. However, this is very unlikely since the temperature was very low (323 K). Heating in the gas mixture fully activates the Au/TiO_2 catalyst. The activity cannot stem from impurities of the colloid preparation procedure, because the zirconia catalyst is less active under the same conditions. Moreover, these results prove that no intimate structural gold/oxide interface is necessary for the low temperature oxidation of CO and they confirm that high dispersion of gold is an additional key factor as postulated in Refs. (5, 6, 30).

Although no strong structural gold/support interaction seems to be necessary, the support plays a crucial role for the low temperature CO-oxidation of gold. This can be concluded from the following observation: The dried Au/ZrO_2 catalyst did not exhibit significant activity at room temperature, although the particle size was similar to that of the titania catalyst and similar to those reported by other authors (5, 6). The investigation of the calcined Au/ZrO_2 and Au/TiO_2 catalysts revealed a similar tendency; titania is superior to zirconia as a support. However, as stated above, in the case of calcined catalysts (especially at higher temperatures) the support can have a great influence on the particle size of gold due to the different wetting ability. Since most of the catalysts prepared via "conventional" preparation procedures were activated by a calcination procedure, these results permit a comparison to previously reported data from catalytic tests. The catalysts presented here show excellent activity in comparison with those prepared by other preparation procedures (4, 5, 31). In a recent work Yuan *et al.* fixed phosphine complexes on the metal oxide surface (32, 33). Interestingly, they did not find significant activity at room temperature when using commercially available metal oxide supports due to strong aggregation of the gold complexes during calcination. They achieved only high conversion if the metal complexes were fixed on as-precipitated gold complexes.

The CO conversion data of the Au/ZrO_2 catalyst prepared via colloids can also be compared to those of a co-precipitated zirconia catalyst as reported by Knell *et al.* (4). The same 1 : 1 CO/O_2 feed gas mixture, a similar CO feed rate, and the same catalyst loading have been used for both investigations. The temperature required for 50% CO-conversion is similar for both kinds of catalysts, showing

that catalysts prepared by the two different methods result in very similar catalytic properties.

Finally, it was shown that the activity of gold-supported titania catalysts depends strongly on the pretreatment and the content of water. Water inhibits the reaction, especially at lower temperatures, probably due to adsorption on active sites or to pore filling (capillary condensation). This phenomenon was also found in other studies (5) and may be the reason for the lower activity of uncalcined gold catalysts at room temperature. Water is removed after heating to 423 K in the reaction mixture, resulting in higher activity after subsequent cooling. The loss of water from the dried catalyst could also be followed by IR-spectroscopy in the gas cell.

5. CONCLUSIONS

The preparation of Au/TiO_2 and Au/ZrO_2 via "size controlled" gold colloids affords highly active catalysts for the low temperature oxidation of CO. Analysis of the gold particles during different stages of the preparation indicated that the size of the gold particles in the colloidal solution is nearly preserved during immobilization. UV-vis spectrophotometry, after comparison with HRTEM data, proved to be a useful *in situ* method to follow the particle size during the different preparation steps in solution. The adsorption of gold colloids at pH < IEP is supposed to occur similar to that of metal complex anions.

Gold particle size and the nature of the support are the major factors controlling the activity of supported gold particles. However, no strong interfacial contact between gold and the oxide, as often postulated, seems to be necessary, as follows from the fact that the uncalcined Au/TiO_2 catalyst shows significant activity. Water in the feed gas lowers the CO-oxidation activity of Au/TiO_2; however, the activity is regained under dry feed gas conditions.

Catalyst preparation via gold colloids offers the possibility to tailor the gold particle size before deposition on various supports. Moreover, this route can also be used for gold immobilization on supports such as Al_2O_3, where conventional preparation methods have considerable limitations. This could give valuable insight into the role of the particle size and further aspects of the mechanism of low temperature CO oxidation. Different nearly monodisperse solutions can be prepared by ageing of the gold colloids, or boiling of the gold sols.

ACKNOWLEDGMENTS

Thanks to O. Becker (Universität Zürich) and R. Wessiken (ETH Hönggerberg) for performing the HRTEM measurements and to P. M. Fabrizioli for helping to perform the UV-vis measurements. We also thank R. A. Köppel for fruitful discussions.

REFERENCES

1. Haruta, M., Kobayashi, T., Tsubota, S., and Nakahara, Y., *Chem. Express* **5**, 349 (1988).
2. Haruta, M., Yamada, N., Kobayashi, T., and Iijima, S., *J. Catal.* **115**, 301 (1989).
3. Tsubota, S., Cunningham, D. A. H., Bando, Y., and Haruta, M., *Stud. Surf. Sci. Catal.* **91**, 227 (1995).
4. Knell, A., Barnickel, P., Baiker, A., and Wokaun, A., *J. Catal.* **137**, 306 (1992).
5. Bollinger, M. A., and Vannice, M. A., *Appl. Catal. B Environm.* **8**, 417 (1996).
6. Haruta, M., *Catal. Today* **36**, 153 (1997).
7. Boccuzzi, F., Chiorino, A., Tsubota, S., and Haruta, M., *Catal. Lett.* **29**, 225 (1994).
8. Frens, G., *Nature Phys. Sci.* **241**, 20 (1973).
9. Roth, J., *in* "Techniques in Immunochemistry, Vol. 1" (G. R. Bullock and P. Petrusz, Eds.), p. 108. Academic Press, London/New York, 1982.
10. Duff, D. G., Baiker, A., and Edwards, P. P., *J. Chem. Soc. Chem. Commun.*, 96 (1993).
11. Duff, D. G., Baiker, A., and Edwards, P. P., *Langmuir* **9**, 2301 (1993).
12. "Mineral Powder Diffraction Data Files." JCPDS-International Center for Diffraction Data, Swarthmore, PA, 1991.
13. Scherrer, P., *Gött. Nachr.* **2**, 98 (1918).
14. Klug, H. P., and Alexander, L. E., "X-Ray Diffraction Procedures for Polycrystalline and Amorphous Materials." Wiley, New York, 1974.
15. Briggs, D., and Seah, M. P., "Practical Surface Analysis by Auger and X-ray Photoelectron Spectroscopy." Wiley, Chichester, 1983.
16. Shirley, D. A., *Phys. Rev. B* **5**, 4709 (1972).
17. Gregg, S. J., and Wing, K. S. W., *Surf. Colloid. Sci.* **9**, 254 (1976).
18. Köppel, R. A., Nickl, J., and Baiker, A., *Catal. Today* **20**, 45 (1994).
19. Radtke, F., Köppel, R. A., and Baiker, A., *Catal. Today* **26**, 159 (1995).
20. Kreibig, U., and Genzel, L., *Surf. Sci.* **156**, 678 (1985).
21. Kirkland, A. I., Edwards, P. P., Jefferson, D. A., and Duff, D. G., *Annu. Rep. Prog. Chem. C* **87**, 247 (1990).
22. Chow, M. K., and Zukoski, C. F., *J. Coll. Interface Sol.* **165**, 97 (1994).
23. Creighton, J. A., and Eadon, D. G., *J. Chem. Soc. Faraday Trans.* **87**, 3881 (1991).
24. Mie, G., *Ann. Phys.* **25**, 377 (1908).
25. Brunelle, J. P., *Pure Appl. Chem.* **50**, 1211 (1978).
26. Kennedey, D. C., *Chem. Eng.* **12**, 186 (1980).
27. Parks, G. A., *Chem. Rev.* **65**, 177 (1965).
28. Handley, D. A., *in* "Colloidal Gold, Vol. 1" (M. A. Hayat, Ed.), p. 1. Academic Press, New York, 1989.
29. Iwasawa, Y., "Tailored Metal Catalysts." Reidel, Dordrecht, 1984.
30. Haruta, M., *in* "3rd World Congress on Oxidation Catalysis" (R. K. Grasselli, S. T. Oyama, A. M. Gaffney, and J. E. Lyons, Eds.), p. 123. Elsevier Science, New York, 1997.
31. Haruta, M., Tsubota, S., Kobayashi, T., Kageyama, H., Genet, M. J., and Delmon, B., *J. Catal.* **144**, 175 (1993).
32. Yuan, Y. Z., Asakura, K., Wan, H. L., Tsai, K., and Iwasawa, Y., *Catal. Lett.* **42**, 15 (1996).
33. Yuan, Y. Z., Kozlova, A. P., Asakura, K., Wan, H., Tsai, K., and Iwasawa, Y., *J. Catal.* **170**, 191 (1997).